Electronic Supplementary Information

Plasmon-assisted nanophase engineering of titanium dioxide for improved performances in single-particle based sensing and photocatalysis

Shuangshuang Wang,[a] Jiacheng Yao,[a] Zhenwei Ou,[a] Xujie Wang,[a] Yinfeng Long, [a] Jing Zhang,[a] Zheyu Fang,[b] Ti Wang,[a] Tao Ding*[a] and Hongxing Xu[a,c]

a. Key Laboratory of Artificial Micro- and Nano-structures of Ministry of Education of China, School of Physics and Technology, Wuhan University, Wuhan 430072, China.
b. School of Physics, State Key Laboratory for Mesoscopic Physics, Academy for Advanced Interdisciplinary Studies, Collaborative Innovation Center of Quantum Matter, Nano-optoelectronics Frontier Center of Ministry of Education, Peking University, Beijing 100871, China
c. School of Microelectronics, Wuhan University, Wuhan 430072, China.

Temperature calculations:

Stationary study and heat transfer in solids interface were employed to calculate the temperature distribution around the AuNP. The heat source (Q) was determined by the absorption cross section of AuNPs in TiO2 (σ_{abs}) and power density of the laser (I_P).

$$Q = \sigma_{abs} * I_P$$

$$I_P = \frac{P_{laser}}{\pi(w_0)^2}$$

Where σ_{abs} is the absorption cross-section of AuNP (determined by FDTD simulation), P_{laser} is the laser power applied in the experiment (1-5 mW), w_0 is the waist radius of the focused laser beam (~270 nm).

The boundary condition is set as a constant temperature of 293.15 K. We use 2D axial symmetric Space dimensions to build 3D geometry. The mesh size of AuNPs and surrounding medium are set as 1 and 10 nm, respectively. The properties of materials are list in the table below:

Matertial	Density [kg/m^3]	Thermal conductivity [W/(m*K)]
Au	19320	318
Si	2329	Built-in function
TiO_2	3894	0.59[1]

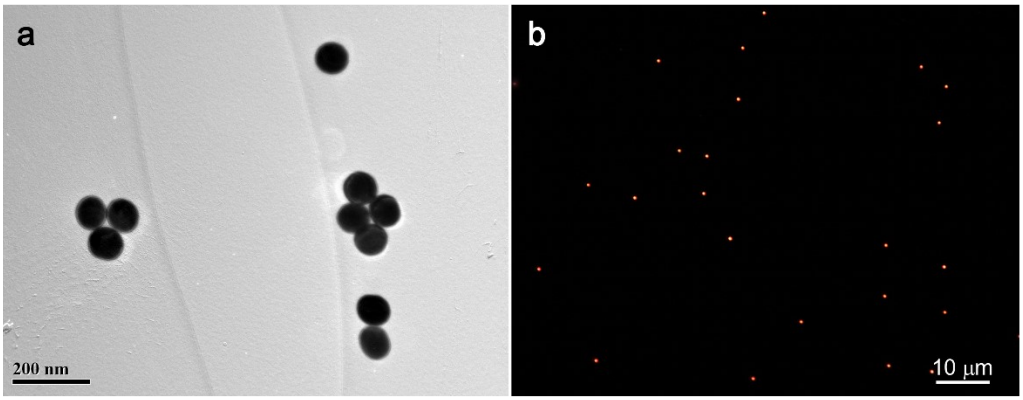

Figure S1. Characterizations of AuNPs. (a) TEM image of the 80 nm AuNPs. (b) Dark filed image of AuNPs on Si substrate coated with TiO_2 thin films.

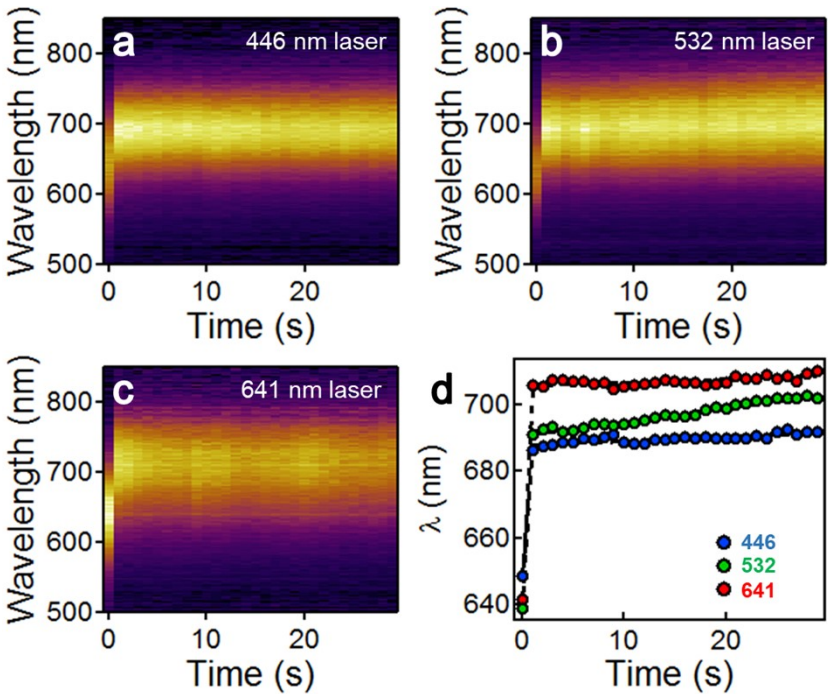

Figure S2. Influence of the irradiation wavelength on the spectral shift of LSPR. (a) 446 nm. (b) 532 nm. (c) 641 nm. (d) Change of LSPR peaks with the irradiation time of different laser wavelengths. The irradiation power density of each wavelength is fixed at 17.5 mW/μm^2.

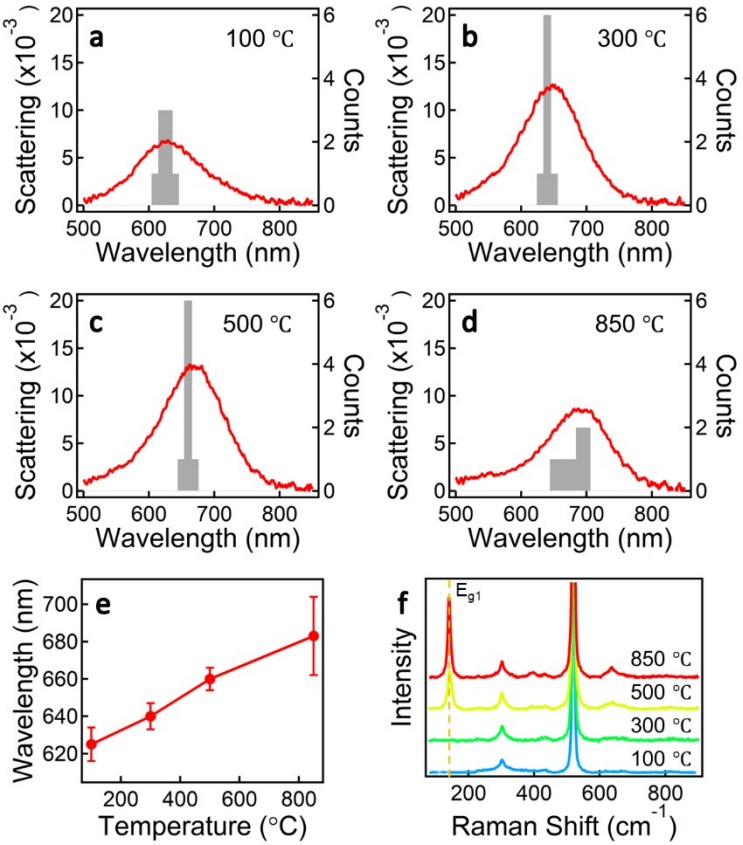

Figure S3. Statistical analysis of DF scattering spectra of AuNPs in TiO_2 films after global annealing at different temperatures for 2 hours: (a) 100 °C; (b) 300 °C; (c) 500 °C; (d) 850 °C. All the spectra are statistically collected and averaged over 8 AuNPs. (e) Change of the LSPR wavelength with temperature. (f) Raman spectra of the TiO_2 films annealed at different temperature. The peak of E_{g1} emerges at 143 cm^{-1} after 500 ˚C annealing and slightly shifted to 140 cm-1 after 850 ˚C annealing.

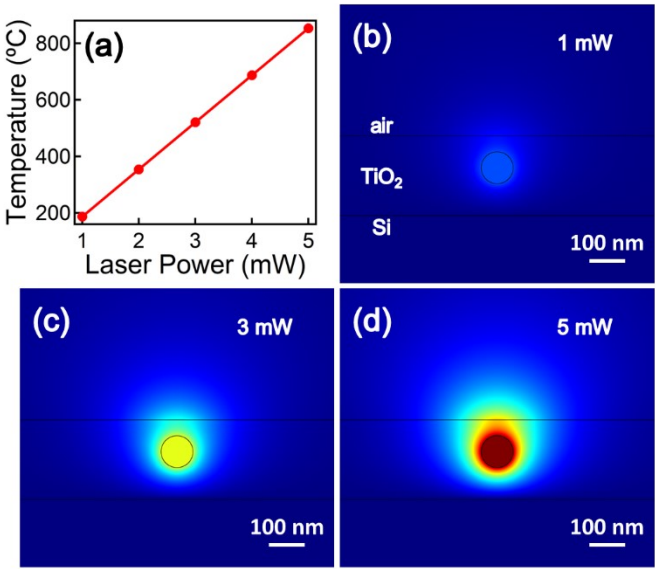

Figure S4. Temperature Simulations of AuNPs embedded in TiO_2 on Si substrate with different laser powers. (a) Change of AuNP surface temperature with laser power. (b-d) Temperature distribution around the AuNP at different laser power: b) 1 mW, c) 3 mW, d), 5 mW.

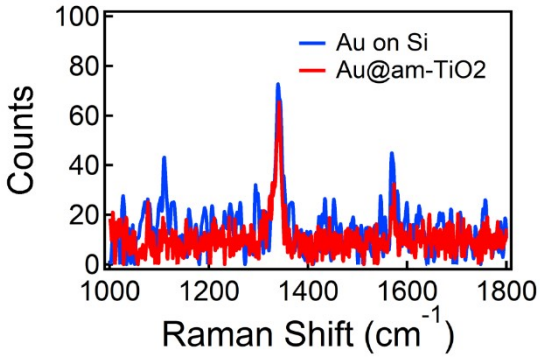

Figure S5. Raman spectra of 4-NBT of AuNPs on Si and embedded in amorphous TiO_2 films.

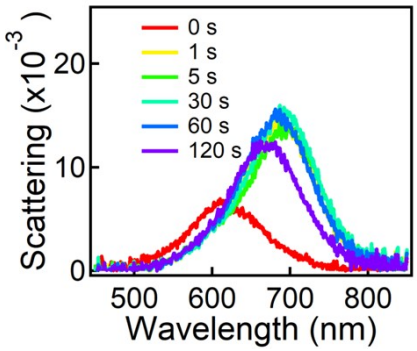

Figure S6. Averaged Scattering spectra of AuNPs annealed at different irradiation times (laser power: 5.5 mW).

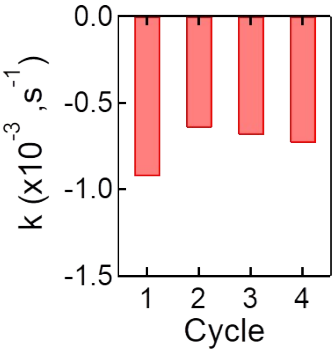

Figure S7. Degradation rate constant of 4-NBT at different cycles of photocatalysis.

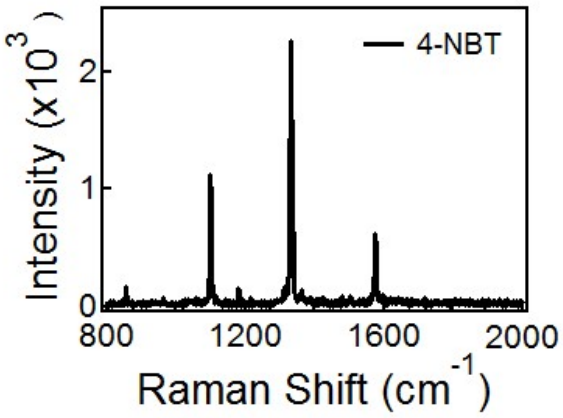

Figure S8. The Raman spectrum of 4-NBT powders.

Reference

1 T. Coquil, C. Reitz, T. Brezesinski, E. J. Nemanick, S. H. Tolbert and L. Pilon, *J. Phys. Chem. C*, 2010, **114**, 12451-12458.